



CT-based weight assessment of lung lobes: comparison with *ex vivo* measurements

Nicola Sverzellati, Jan-Martin Kuhnigk, Simone Furia, Stefano Diciotti, Paolo Scanagatta, Alfonso Marchianò, Francesco Molinari, Christina Stoecker, Ugo Pastorino

PURPOSE

We aimed to evaluate the validity of lung lobe weight assessment via computed tomography (CT) by comparing CT-derived and *ex vivo* measurements.

MATERIALS AND METHODS

Unenhanced CT scanning was performed in 30 consecutive patients before lobectomy for lung cancer. The CT images were analyzed using research software after allowing for lobar weight quantitation. The lobar weight estimated by CT was then compared with that measured after surgery using a precision scale (*ex vivo* measurement). Comparisons as well as assessment of intra- and interoperator variability were conducted using the Bland-Altman method and the coefficient of repeatability (CR). Correlations were examined using Pearson's correlation analysis.

RESULTS

Comparison analyses were feasible for 28 cases. The *ex vivo* lobe weight was 186.2 ± 57.3 g, whereas the weights measured by the two operators by CT were 190.0 ± 55 and 182.4 ± 58.2 g, respectively. As compared with *ex vivo* weights, the CR was 36.4 for operator 1 and 50.4 for operator 2; the mean differences were 3.8 and -3.8 for operators 1 and 2, respectively. The intraoperator and interoperator CR were 20.9 and 36.6, respectively. The mean differences for the intra- and interoperator analysis were -1.5 and -7.5, respectively. The correlation was very high between CT-based and *ex vivo* measurements ($r=0.95$ and $r=0.90$ for operators 1 and 2, respectively; $P < 0.001$).

CONCLUSION

Estimation of lung lobe weight by semi-automated CT analysis is sufficiently reproducible and in agreement with *ex vivo* measurements.

Computed tomography (CT) is the most widely used imaging modality for the evaluation of lung disease at the lobar level. Several methods for the automatic and semi-automatic segmentation of the lung lobes have been developed (1–5).

This advance in postprocessing CT technique also allows lobar assessment of several CT parameters, such as volume, mean density, and emphysema extent. Lobe-specific measurements may provide insight into both underlying disease mechanisms and the spectrum of disease phenotypes (particularly in chronic obstructive lung disease), as well as help to refine therapeutic strategies (4–6). Prior studies also evaluated the reliability of the corresponding measurements by testing the inherent interoperator variability or comparing software results with the visual score (7, 8). However, the accuracies of CT-based lobe segmentation and measurements have yet to be proven in comparison with a gold standard, such as pathological measurements.

The combination of lung volume and density allows the estimation of other volumetric parameters such as lung weight (9, 10). The lobe weight when assessed by automated CT analysis may be suitable for pathological correlations. Lobe weight measurement, as outlined in the present study, is based on the calculation of lobe density and volume. Lobe volume variation (e.g., due to different levels of inspiration) may be attenuated using the density of the corresponding lung. Therefore, weighing the lungs by CT may be important because such a measurement is likely less affected by inspiration depth, and could replace other parameters for assessment of the evolution of several lung diseases (10).

In this study, we evaluated the validity of lung lobe weight assessment via CT by comparing CT-derived and *ex vivo* measurements.

Materials and methods

The Institutional Review Board approved this prospective study and waived the need for the informed consent. The study population consisted of 30 patients (18 males, 12 females; age range, 49–79 years; and mean age, 66.2 ± 8.2 years for males; age range, 46–74 years; and mean age, 61.9 ± 9.5 years for females) who underwent lobectomy for lung cancer at the section of thoracic surgery of the Fondazione IRCCS Istituto Nazionale dei Tumori (Milan, Italy); 13 right upper lobectomies, seven left upper lobectomies, three left lower lobectomies, two combined right lower and middle lobectomies, two right lower lobectomies, two middle lobectomies, and one combined right upper and middle lobectomy.

After surgery, each removed lobe (including the tumor) was weighed on a precision scale (PM30-K, Mettler, Toledo, Italy) by one of two thoracic surgeons (S.F. and P.S., with seven and nine years of experience in thoracic surgery, respectively). The weight (grams, g) measurements (*ex vivo* weights) were recorded (Fig. 1a).

From the Department of Clinical Sciences (N.S. ✉ nicola.sverzellati@unipr.it), Section of Diagnostic Imaging, University of Parma, Parma, Italy; Fraunhofer MEVIS (J.M.K., C.S.), Bremen, Germany; Department of Surgery (S.F., P.S., U.P.), Thoracic Section, Fondazione IRCCS Istituto Nazionale dei Tumori, Milan, Italy; Computational Biomedical Imaging Laboratory (S.D.), Radiodiagnostic Section, Department of Clinical Physiopathology, University of Florence, Florence, Italy; Division of Radiology (A.M.), Fondazione IRCCS Istituto Nazionale dei Tumori, Milan, Italy; C. H. R. U. Lille (F.M.), Hôpital Calmette, Lille, France.

Received 22 November 2012; revision requested 16 December 2012; revision received 28 February 2013; accepted 4 March 2013.

Published online 3 June 2013.
DOI 10.5152/dir.2013.149

All study patients underwent whole-body CT scanning for disease staging one week before surgery. Scanning was performed using a 16-detector row CT scanner (Somatom Sensation 16, Siemens Medical Solutions, Forchheim, Germany). The scanner was daily calibrated on air to allow reliable comparisons between examinations.

The CT protocol included one thin-section CT scan of the whole lung during one deep inspiratory breath-hold without the use of contrast medium. The CT parameters were as follows: kVp, 120; effective mAs, 100; individual detector collimation, 0.75 mm; gantry rotation time, 0.5 s; and pitch, 1.5. For each CT examination, images were reconstructed in 1 mm thick sections with a reconstruction increment of 1 mm (medium-sharp kernel B50f). This CT scan was then used for the postprocessing computer analysis of the lung lobes.

Software analysis

Each set of CT images was analyzed using research software (MeVisPULMO 3D®, v3.071, Fraunhofer MEVIS, Bremen, Germany) by two operators (N.S. and J.M.K., with seven and six years of experience in postprocessing CT quantitative analysis of the lungs, respectively) on different occasions and using different personal computers. After two months, the first operator blinded to his previous measurements, repeated the analyses on the same subjects for assessment of the intraobserver agreement.

In medium-sharp kernel images, noise was further reduced by application of a 3×3 kernel-based axial Gaussian smoothing. The software algorithm was detailed previously (1, 7). Briefly, the software automatically excluded bone and soft tissues using a density mask of -400 Hounsfield unit (HU), separated the lungs from the tracheo-bronchial tree and other nonpulmonary structures, and segmented the lobes. The lobes were identified using lung vessels as anatomic landmarks. The segmentation of the pulmonary vasculature was restricted to the area defined by the previously computed lung masks and was performed using a conventional three-dimensional region-growing algorithm, thereby creating a superset

of all larger pulmonary vessels. Accordingly, lobar segmentation was based on the absence of larger vessels in proximity to the lobar boundaries. For this purpose, an Euclidean distance transform was used, and lobar areas were obtained from the preprocessed image using a multidimensional interactive watershed transform. Initial lobe labels of the watershed regions were automatically derived from the lobar subtrees in the segmented bronchial tree. These initial results were provided for interactive correction by the operators using color-coded overlays on axial, coronal, and sagittal CT images (Fig. 1b). Thereby, the segmentation could be iteratively refined until the lobes were identified correctly. Semi-automated segmentation required approximately 10 min per case. The frequency of manual interaction for lobes segmentation was recorded by the first operator.

These region identification steps enabled extraction of various CT parameters, such as volume, mean density, pixel index, bulla index, and emphysema type on a lobar basis. Assuming a close relationship between radiodensity (i.e., mean density) and mass density, the combination of lung volume and density allowed lung weight (g) estimation using the following formula: $\text{Weight (g)} = \text{volume (mL)} \times (\text{mean density [HU]} + 1000 \text{ HU}) / 1000$

For the experiments, the weight of the lung lobe that was subject to resection was recorded.

The first operator also measured the maximal diameter of the lung cancer and recorded whether the lung cancer or associated atelectasis was automatically excluded by the segmentation process (which can happen if the smallest tumor diameter is >2 cm). In addition, the same operator recorded the presence

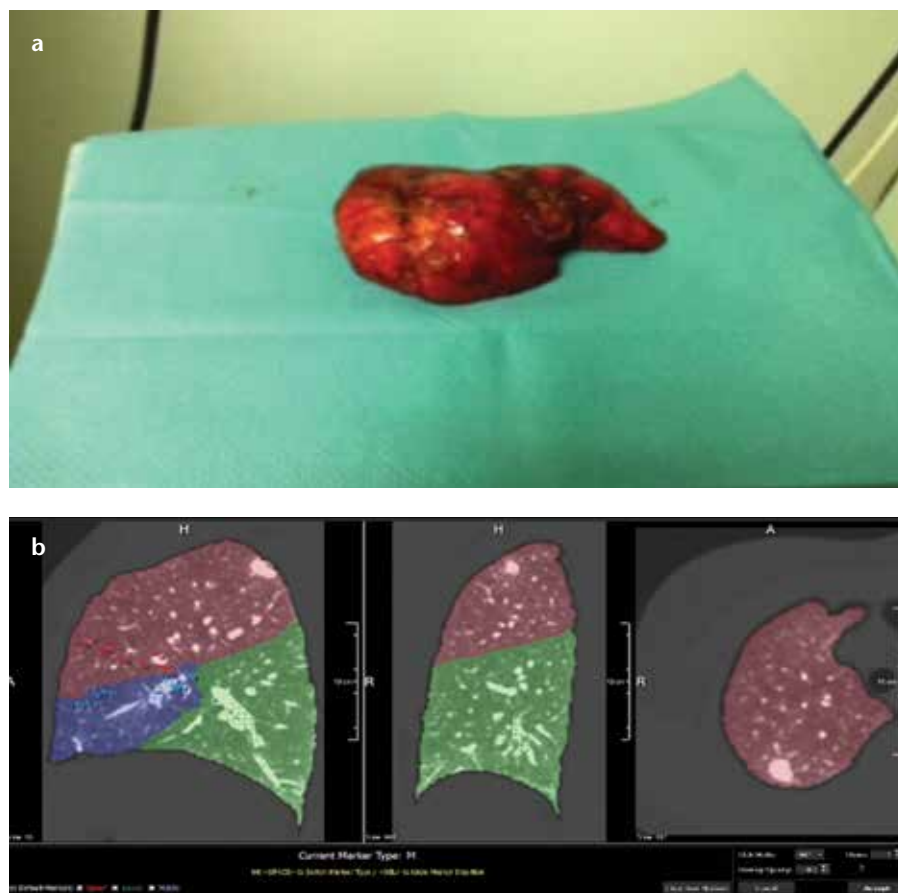


Figure 1. a, b. The study procedure as followed in one male smoker with an adenocarcinoma in the right upper lobe. After resection (a), the right upper lobe was weighed on a precision scale (Mettler, PM30-K), and the corresponding measurement was recorded. User interface of the software during verification and refinement of the right upper lobar segmentation (b) are shown. The segmented regions are represented by colored overlays on sagittal (left), coronal (middle), and axial (right) images.

of any accessory or incomplete fissure within the target lobe. Cases with an accessory fissure, large atelectasis, or large tumor preventing the lobe segmentation were excluded from the analysis.

Statistical analysis

A paired *t* test was used to evaluate differences between CT-based and corresponding *ex vivo* weights. The agreement between CT-based and corresponding *ex vivo* weights was examined using the Bland-Altman method in terms of mean difference and 95% limits of agreement (11). The intra- and interoperator agreements between CT-based measurements were also evaluated using the Bland-Altman method (11). For all of the agreement analyses, the coefficient of repeatability (CR), defined as 1.96 times the standard deviation of the differences between two sets of measurements, was also calculated. For the 95% limits of agreement and CR computation, the difference between the two measurements was required to be unrelated to the magnitude of the measurements. For this reason, the Kendall *t* test with $P < 0.05$ was preliminarily applied to each agreement analysis to evaluate the correlation between the standard deviation and the magnitude of lobar weights. In the case of a significant correlation, a log-transformation of the data was applied and, accordingly, 95% limits of agreement and mean differences were converted to percentage values of the original measurements (11).

Correlations between CT-based and *ex vivo* measurements were evaluated using Pearson's correlation coefficient.

All statistical analyses were performed using Matlab (MathWorks, version 7, Natick, Massachusetts, USA).

Results

The lobe segmentation could not be finalized for one case with an accessory fissure in the target lobe. Another case could not be evaluated by one operator (J.M.K.) due to technical reasons (i.e., error in data transfer). Therefore, 28 patients (17 males, 11 females; age range, 49–79 years; and mean age, 67.2 ± 7.2 years for males; age range, 46–74 years; and mean age, 61.3 ± 9.7 years for females) were considered for comparative

analyses. The *ex vivo* lobe mean weight was 186.2 ± 57.3 g, whereas those measured by the two operators by CT were 190.0 ± 55 and 182.4 ± 58.2 g, respectively. There was no significant difference between CT-based and *ex vivo* measurements ($P = 0.29$ and $P = 0.45$ for operators 1 and 2, respectively).

An incomplete fissure was observed in one case in which a sizeable discrepancy between *ex vivo* and computer-based analysis was reported for one operator (38 g for one operator, and 6 g for the other). In one patient who underwent bilobectomy (resection of both right upper lobe and middle lobe), the tumor was endobronchial, and its diameter was not measured. The mean tumor size in the remaining 27 patients was 2.9 ± 1.3 cm. One patient had a completely cavitated tumor 7.1 cm in size, whereas in another patient a 3.8 cm tumor appeared partly cavitated.

CT-based and *ex vivo* measurements were highly correlated ($r = 0.95$ and $r = 0.90$, for operators 1 and 2, respectively;

$P < 0.001$). No significant correlation between the difference in measurements and their magnitude was observed in the case of CT-derived and *ex vivo* weights for both operators ($P = 0.92$ and $P = 0.65$, respectively). No significant correlation was found in the intra- and interoperator agreement analysis ($P = 0.70$ and $P = 1.00$, respectively). Since no correlation between the difference and magnitude of measurements was significant, the Bland-Altman analyses were performed on the original measurement scale.

When compared with *ex vivo* weights, the CRs were 36.4 for operator 1 and 50.4 for operator 2; the mean differences were 3.8 and -3.8 for operators 1 and 2, respectively (Table and Fig. 2).

The intra- and interoperator CRs were 20.9 and 36.6, respectively. The mean differences were -1.5 and -7.5 for the intra- and interoperator analyses, respectively (Table and Fig. 3). The Bland-Altman 95% limits of agreement are shown in Table.

Table. Bland-Altman analyses of CT-estimated lobar weight measurements

	Mean difference (g)	95% limits of agreement (g)	CR
Comparison with <i>ex vivo</i> weights			
Operator 1 vs. <i>ex vivo</i> weights	3.8	-32.6 to 40.1	36.4
Operator 2 vs. <i>ex vivo</i> weights	-3.8	-54.5 to 47.0	50.4
Intraoperator agreement (operator 1)			
Session 1 vs. session 2	-1.5	-22.6 to 19.6	20.9
Interoperator agreement			
Operator 1 vs. operator 2	-7.5	-41.6 to 26.5	36.6

CR, coefficient of reproducibility.

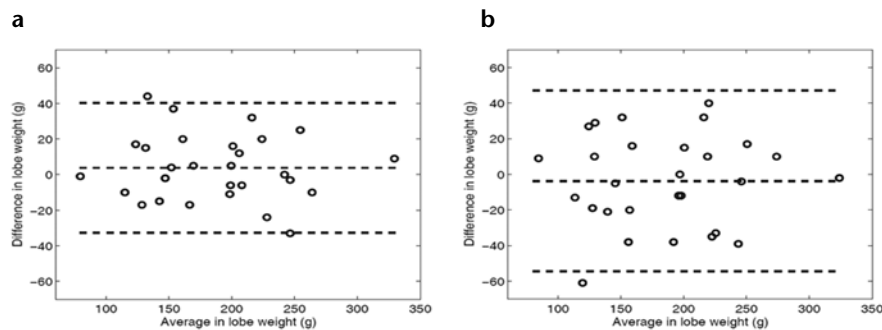


Figure 2. a, b. Bland-Altman plots showing the means and differences between lobar weights measured by CT and *ex vivo* for operator 1 (a) and operator 2 (b).

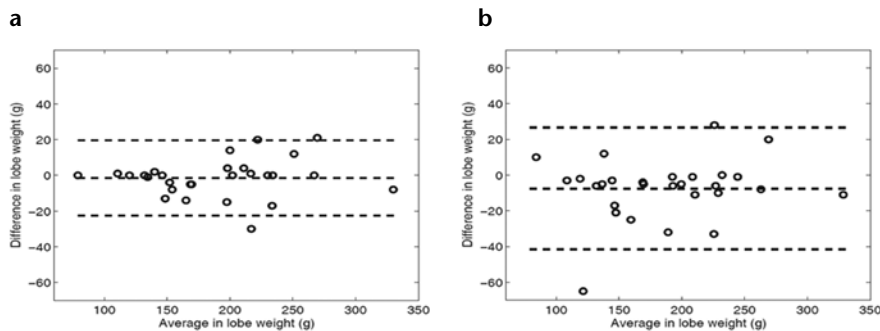


Figure 3. a, b. Bland-Altman plots showing the means and differences between lobar weights measured by CT and *ex vivo* for both the intraoperator analysis of the operator 1 (a), and the interoperator analysis (b).

Although the tumor was completely or partly excluded in four and eight subjects, respectively, this factor did not appear to be related to the differences between CT and *ex vivo* measurements for both operators. Thus, after exclusion of these cases, the CRs remained unchanged (38.6 for operator 1 and 51.8 for operator 2).

Discussion

The present study was designed to assess the validity of CT-based lobe segmentation and quantitation. Accordingly, we defined the ranges of reproducibility and showed that CT-estimated lobe weight is comparable to that measured *ex vivo*.

Although the degree of interoperator variability that is acceptable for clinical applications is uncertain, the lobe weight quantitation was not affected by any substantial inter- or intraoperator variability. This was true despite the frequent need for minor manual interventions to optimize lobe segmentation. This result is in accordance with a recent study of the interoperator agreement that used the same software (12). Conversely, this result partly contradicts another study in which the authors used a different software model that allowed only manual segmentation of the lobes, which indicates that the segmentation method used affects the reproducibility (8).

Several previous studies showed the potential usefulness of CT-based lung weight measurements. The lung weight assessed by automated CT was calculated by multiplying the lung density by its volume (9, 10). In one

study, the CT total lung weight measurements of 35 children compared favorably to published postmortem values (9). Quantitative CT was also reported to enable objective tracking of the changes in lung weight and airspace inflation produced by a standard intervention, as in pulmonary alveolar proteinosis (10). The present study is the first to specifically address the validity of assessment of lobe weight by semi-automated CT analysis. We applied an analytic methodology similar to that used for comparison of CT-based and histological morphometric measurements of pulmonary emphysema (13, 14). The mean differences between CT and *ex vivo* measurements were low. The CR value confirmed that CT measurements adequately reflect the range of the *ex vivo* measurements. Our results suggest the value of CT-based densitometric measurements; these could be used in future studies as *ex vivo* surrogate indices for comparative analyses.

Therefore, lobe-specific analysis by CT may provide important advantages particularly for the longitudinal assessment of lung weight in patients with several types of progressive lung disease, such as acute respiratory distress syndrome. Thus, in contrast to the sole lung density, lung and lobe weights measured by CT may be unaffected by inspiration depth. The pathological processes assumed to be associated with weight increases (e.g., lung inflammation and fibrosis) can be followed up and quantified even if the inspiration level differs substantially between examinations.

Our study has several limitations. The study cohort was not sufficiently large to allow determination of whether the correlation between CT-based and *ex vivo* weight measurements, as well as interoperator agreement, varied among pulmonary lobes. Anecdotally, the right upper lobe was the target lobe that usually required more manual intervention for optimization of the virtual segmentation process. The software could not assess the entire lung tumor in some cases; this constitutes the major limitation of the tested version of this software. Nevertheless, the differences between the software and *ex vivo* measurements were not definitively linked to the exclusion of some tumors. Since we could not weigh the tumor separately, its contribution to the total weight could not be predicted. Additionally, it was not possible to ascertain that the blood volume within the lobes remained constant, whether measured *ex vivo* or by CT. Furthermore, the *ex vivo* measurements could not be regarded as a gold standard because a minimal loss of blood after surgery, which would reduce the weight of the lung, cannot be excluded.

In conclusion, estimation of lung lobe weight by semi-automated CT analysis is sufficiently reproducible and in agreement with *ex vivo* measurements.

Conflict of interest disclosure

The authors declared no conflicts of interest.

References

1. Kuhnigk JM, Dicken V, Zidowitz S, et al. Informatics in radiology (infoRAD): new tools for computer assistance in thoracic CT. Part 1. Functional analysis of lungs, lung lobes, and bronchopulmonary segments. *Radiographics* 2005; 25:525–536. [\[CrossRef\]](#)
2. Wei Q, Hu Y, Gelfand G, Macgregor JH. Segmentation of lung lobes in high-resolution isotropic CT images. *IEEE Trans Biomed Eng* 2009; 56:1383–1393. [\[CrossRef\]](#)
3. Zhang L, Hoffman EA, Reinhardt JM. Atlas-driven lung lobe segmentation in volumetric X-ray CT images. *IEEE Trans Med Imaging* 2006; 25:1–16. [\[CrossRef\]](#)
4. Busacker A, Newell JD Jr, Keefe T, et al. A multivariate analysis of risk factors for the air-trapping asthmatic phenotype as measured by quantitative CT analysis. *Chest* 2009; 135:48–56. [\[CrossRef\]](#)

5. Matsuo K, Iwano S, Okada T, Koike W, Naganawa S. 3D-CT lung volumetry using multidetector row computed tomography: pulmonary function of each anatomic lobe. *J Thorac Imaging* 2012; 12:164–170. [\[CrossRef\]](#)
6. Sverzellati N, Calabro E, Randi G, et al. Sex differences in emphysema phenotype in smokers without airflow obstruction. *Eur Respir J* 2009; 33:1320–1328. [\[CrossRef\]](#)
7. Revel MP, Faivre JB, Remy-Jardin MD, et al. Automated lobar quantification of emphysema in patients with severe COPD. *Eur Radiol* 2008; 18:2723–2730. [\[CrossRef\]](#)
8. Molinari F, Amato M, Stefanetti M, et al. Density-based MDCT quantification of lobar lung volumes: a study of inter- and intraobserver reproducibility. *Radiol Med* 2010; 115:516–525. [\[CrossRef\]](#)
9. de Jong PA, Nakano Y, Lequin MH, et al. Estimation of lung growth using computed tomography. *Eur Respir J* 2003; 22:235–238. [\[CrossRef\]](#)
10. Perez At, Coxson HO, Hogg JC, Gibson K, Thompson PF, Rogers RM. Use of CT morphometry to detect changes in lung weight and gas volume. *Chest* 2005; 128:2471–2477. [\[CrossRef\]](#)
11. Bland JM, Altman DG. Statistical methods for assessing agreement between two methods of clinical measurement. *Lancet* 1986; 1:307–310. [\[CrossRef\]](#)
12. Molinari F, Pirroni T, Sverzellati N, et al. Intra- and interoperator variability of lobar pulmonary volumes and emphysema scores in patients with chronic obstructive pulmonary disease and emphysema: comparison of manual and semi-automated segmentation techniques. *Diagn Interv Radiol*. 2013 Nov 27. doi: 10.5152/dir.2013.047. [Epub ahead of print]
13. Gevenois PA, De Vuyst P, de Maertelaer V, et al. Comparison of computed density and microscopic morphometry in pulmonary emphysema. *Am J Respir Crit Care Med* 1996; 154:187–192. [\[CrossRef\]](#)
14. Madani A, Van Muylem A, de Maertelaer V, Zanen J, Gevenois PA. Pulmonary emphysema: size distribution of emphysematous spaces on multidetector CT images--comparison with macroscopic and microscopic morphometry. *Radiology* 2008; 248:1036–1041. [\[CrossRef\]](#)